Influence of Mass Transfer in Distillation: Feasibility and Design

R. Baur and R. Krishna
Dept. of Chemical Engineering, University of Amsterdam, 1018 WV Amsterdam, The Netherlands

R. Taylor
Dept. of Chemical Engineering, Clarkson University, Potsdam, NY 13699

DOI 10.1002/aic.10328
Published online in Wiley InterScience (www.interscience.wiley.com).

The influence is considered of mass transfer on distillation column design. The column design equations incorporating mass-transfer effects are similar to the conventional design equations and are as easy to solve numerically. Mass-transfer effects do not influence pinch-point curves and pitchfork distillation boundaries. Mass transfer does, however, change the composition trajectories, which might thus cross the pinch-point curves. Inclusion of mass transfer in the design equations allows us to estimate the actual number of stages (or the column height). The curvature of composition trajectories may have a significant impact on the total number of stages and on the feed stage location. Mass-transfer effects do not influence the minimum reflux for columns involving a very sharp split. However, and contrary to previous reports, mass-transfer effects may strongly affect the minimum reflux for less than very sharp separations. Mass-transfer effects should be taken into consideration when trace components are a concern. A feasible design based on residue curve maps might be rejected by a design method based on mass transfer. More important, however, the converse also is true. © 2005 American Institute of Chemical Engineers *AIChE J,* 51: 854–866, 2005
Keywords: distillation, mass transfer, feasibility, design

Introduction

The engineer designing a column for the separation by distillation of a multicomponent mixture is interested in knowing the number of stages needed to accomplish a desired separation, where to introduce the feed(s), and certain key operational quantities of which the reflux and reboil ratios are, perhaps, the most important. Graphical methods for the design of columns in the service of binary systems can be found in standard textbooks (for example, Seader and Henley[1]). Analytical and numerical methods for multicomponent systems have also been well established.[1] Over the last two decades elegant graphical and analytical methods for the design of multicomponent distillation systems have been developed (for a comprehensive treatment of the modern approach see the text of Doherty and Malone[2]). These more modern methods feature the use of residue curve (or distillation line) maps, pinch-point curves, and feasible regions.[2,3]

With very few exceptions the methods cited above use equilibrium (stage) models. Real distillation processes, however, nearly always operate away from equilibrium, a fact that has long been recognized, of course. Indeed, it is possible to simulate distillation as a mass-transfer rate-based operation using so-called *nonequilibrium* (NEQ) or *rate-based* models.[4] Although it is obvious that departures from equilibrium will affect the height of a distillation column (the number of stages), it is less clear whether mass-transfer limitations also affect the relative location of the feed(s), the

Correspondence concerning this article should be addressed to R. Taylor at taylor@clarkson.edu.

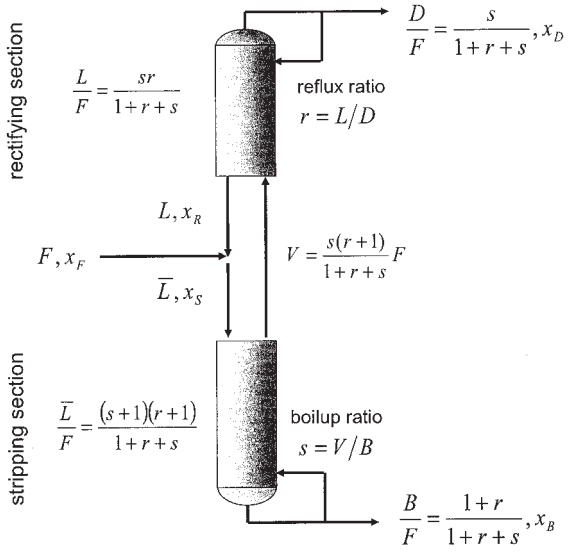

Figure 1. Rectifying and stripping sections of a simple distillation column.

minimum reflux and reboil ratios, the location of pinch points, and column feasibility.

Agarwal and Taylor[5] found, on the basis of simulations, that the minimum reflux ratio for a column with an infinite number of stages was the same whether determined using either a nonequilibrium model or an equilibrium model. However, the models could give very different estimates of the minimum reflux ratio for columns with a specified number of stages. Castillo and Towler[6] used this observation as the basis for their conclusion that mass transfer does not change the pinch points. Castillo et al.[7] looked at how mass transfer can change distillation process feasibility.

It is the aim of this paper to revisit the question of how mass transfer influences distillation process feasibility and design. We shall show that there can be a significant influence of mass transfer on column height (*that does not always lead to an increase in the height*), the location of the feed(s), and process feasibility. Thus, the simple design equations introduced in this paper can serve as a tool to assess the risk of over- or under-design caused by mass-transfer limitations. Furthermore we show that, under circumstances not recognized by Castillo et al.,[5] mass transfer can indeed affect the minimum reflux/reboil ratios. We shall also demonstrate that consideration of mass-transfer limitations can lead to other more effective designs. To avoid confusion, we emphasize that this does not imply that designs based on residue curve maps would not be successful, only that they might be less efficient.

Composition Profiles in Distillation

Consider the simple distillation column shown schematically in Figure 1. We assume constant molar overflow and a saturated liquid feed. Thus, the molar vapor flow V is constant and the liquid flows in the rectifying and stripping section are related by $\bar{L} = L + F$. As shown in Figure 1 we can express the flows in the stripping and rectifying section in terms of the feed flow rate F, the reflux ratio r, and boil-up (reboil) ratio s.

With the help of these results we may write the component mass balance for the whole column in terms of s and r as

$$\frac{r+1}{s}=\frac{x_{i,F}-x_{i,D}}{x_{i,B}-x_{i,F}}=\sqrt{\frac{|(x_F)-(x_D)|}{|(x_B)-(x_F)|}} \tag{1}$$

The last part of Eq. 1 is the ratio of the lengths of two composition vectors: the distance between feed composition (x_F) and the distillate composition (x_D), and the distance between the feed composition (x_F) and the bottom product composition (x_B). It is worth noting that Eq. 1 correlates the reflux ratio with the boil-up ratio for a design problem where the feed and product compositions are specified.

The component material balances for any single stage in the column can be written in matrix form as

$$(x_L - x_E) = \Lambda(y_L - y_E) \tag{2}$$

where the subscripts E and L refer to the streams entering and leaving a stage and where Λ is the local ratio of vapor to liquid flow rates [$\Lambda = V/L = (r + 1)/r$ in the rectifying section and $\Lambda = V/\bar{L} = s/(s + 1)$ in the stripping section]. We may approximate the composition change in the liquid phase by a derivative with respect to a stage number η as

$$(x_L - x_E) = \frac{\Delta(x)}{\Delta\eta} \approx \frac{d(x_L)}{d\eta} \tag{3}$$

We could, of course, do exactly the same thing with the composition change in the vapor phase. However, we also know that the change in the composition of the vapor is given by (cf. Eq. 22 in Taylor et al.[8])

$$(y_L - y_E) = [\Omega](y^* - y_E) \tag{4}$$

where (y^*) is the matrix of mole fractions of a vapor in equilibrium with the liquid of composition (x_L) and where

- For equilibrium stages and residue curves

$$[\Omega] = [I] \tag{5}$$

- For tray columns

$$[\Omega] = [I] - [Q] \qquad [Q] = \exp(-[\mathbb{N}_{OV}]) \tag{6}$$

- For packed columns

$$[\Omega] = [\mathbb{N}_{OV}] \tag{7}$$

These formulas for tray and packed distillation columns rest on the following assumptions:

- The resistance to mass transfer in the liquid phase is totally negligible.
- The molar flows in the column are constant (this requires the latent heats to be equal and the sensible heat fluxes to be negligible in comparison to the enthalpy fluxes).
- The temperature of the system is the bubble-point temperature of the liquid phase.

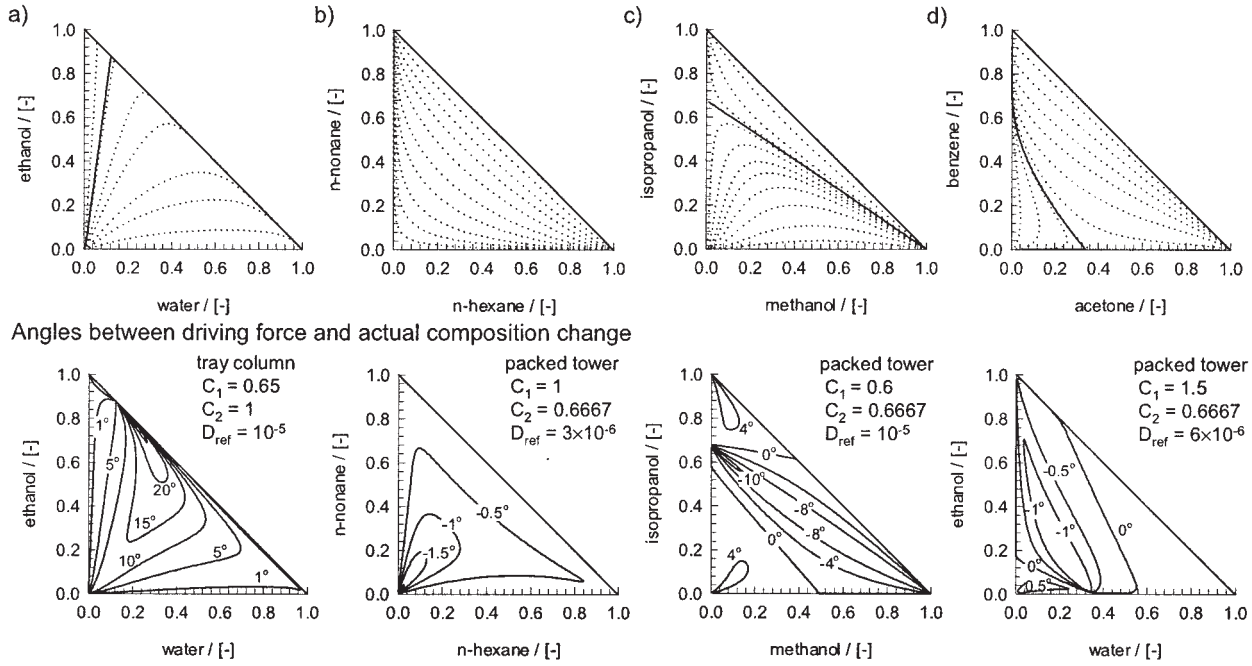

Figure 2. Residue curve maps (top row) and angle maps (bottom row) for the mixture under consideration.

(a) ethanol–water–acetone; (b) hexane–heptane–nonane; (c) methanol–isopropanol–water; (d) acetone–benzene–chloroform.

The calculation of the matrix of numbers of transfer units is described in detail by Taylor and Krishna.[9] For consistency with our earlier work we use Eqs. 33 and 34 from Taylor et al.[8] with the binary numbers of transfer units estimated from

$$\mathcal{N}_{i,j} = C_1 \left(\frac{D_{i,j}}{D_{ref}} \right)^{C_2} \tag{8}$$

The influence of various mixture physical properties, column design, and operational variables are lumped into C_1. The constant C_2 is a parameter of the system and the hydrodynamic regime in the column. We will later assign numerical values to these parameters (see also Taylor et al.[8]). Diffusion coefficients are estimated using methods described in Chapter 4 of Taylor et al.[8]

The composition of the vapor entering the stage can be eliminated with the aid of the material balances from our arbitrary stage to the top of the column

$$(y_E) = \frac{r}{r+1}(x_L) + \frac{1}{r}(x_D) \tag{9}$$

We may now rewrite Eq. 2, with the aid of Eqs. 3–9 as

$$\frac{d(x_L)}{d\eta} = [\Omega]\left((x_L) - \frac{r+1}{r}(y^*) + \frac{1}{r}(x_D) \right) \tag{10}$$

We can derive a similar expression for the composition change in the liquid phase in the stripping section:

$$\frac{d(x_L)}{d\eta} = [\Omega]\left((x_L) - \frac{s}{s+1}(y^*) + \frac{1}{s+1}(x_B) \right) \tag{11}$$

If we assume $[\Omega] = [I]$ (for an equilibrium stage operation) Eq. 10 simplifies to Eq. 5.14 for packed columns of Doherty and Malone.[2] Furthermore, if we use Eq. 3 in reverse we obtain a generalization of their Eq. 5.15 for stage columns. At total reflux/reboil ($r \to \infty$; $s \to \infty$) Eqs. 10 and 11 simplify to

$$\frac{d(x_L)}{d\eta} = [\Omega](x_L - y^*) \tag{12}$$

When $[\Omega] = [I]$ the solutions to Eq. 12 provide the residue curve map (RCM). Thus, mass-transfer effects do not change the basic structure of the RCM. Differences between residue curves and composition trajectories in nonequilibrium distillation operations are characterized by the relative length of and angle between the two composition vectors. As shown by Taylor et al.,[8] the relative length of the composition vectors can be thought of as an average efficiency of a mixture. For tray and packed columns this new definition of efficiency has a simple and appealing physical significance; it is the ratio of the arc lengths of the composition trajectory to the arc length of the corresponding residue curve. For a binary system in a tray column this geometric efficiency is equal to the component Murphree efficiencies. For a binary system in a packed column the geometric average efficiency is the overall number of transfer units.

Figure 2 shows residue curves and composition angle diagrams for the four different ternary systems that we encounter herein: ethanol/water/acetone, *n*-hexane/*n*-heptane/*n*-nonane, methanol/isopropanol/water, and acetone/benzene/chloroform. The angle diagram for the first of these systems is for a tray-column model; the latter three for a packed-column model.

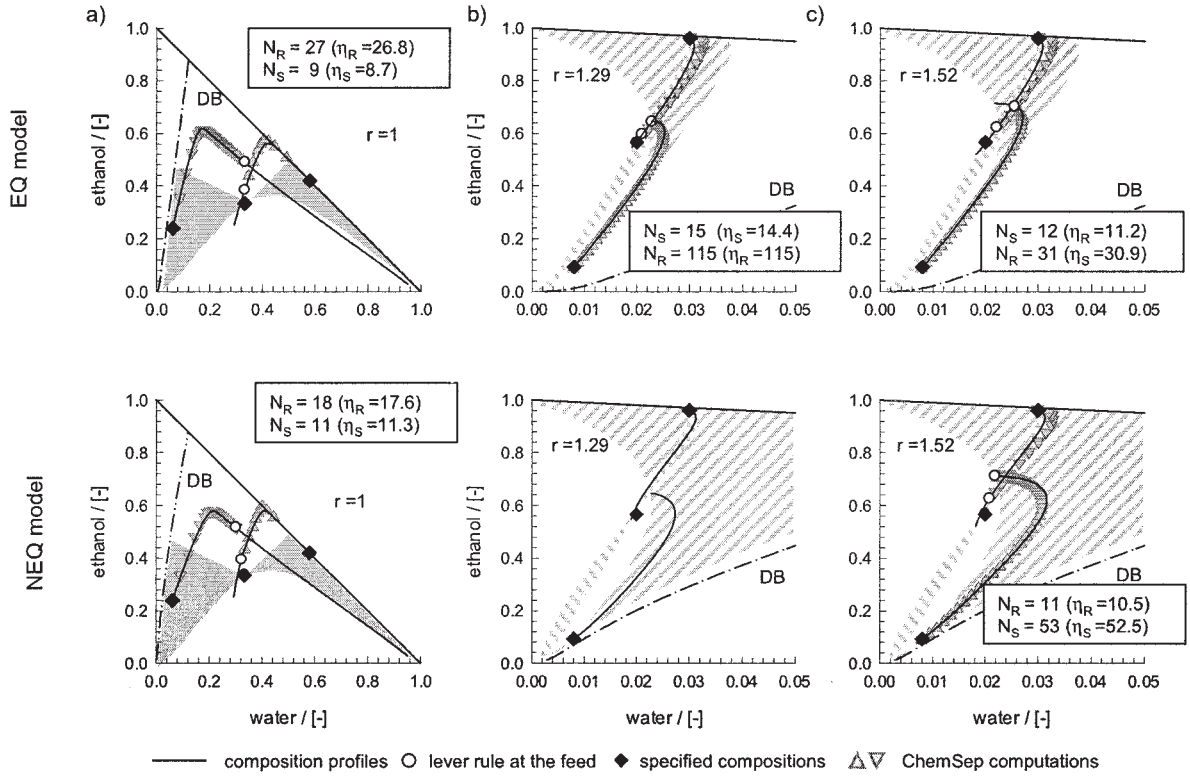

Figure 3. Column designs for ethanol (1)–water (2)–acetone (3).

Figures in the top row show designs based on residue curves, whereas designs based on composition trajectories are shown in the bottom row. The mass-transfer model is based on a tray model ($Đ_{ref} = 10^{-5}$ m^2/s, $C_1 = 0.65$, and $C_2 = 1$). The specified feed and product stream compositions: (a) $(x_D) = (0.061, 0.249)$, $(x_F) = (0.333, 0.333)$, $(x_B) = (0.580, 0.489)$; (b–c) $(x_D) = (0.008, 0.092)$, $(x_F) = (0.02, 0.546)$, $(x_B) = (0.03, 0.96)$. The gray area in (a) denotes the feasible product region for the feed, (x_F). The hatched areas in (b–c) denote the operation leaves for the product stream compositions, (x_D) and (x_B).

Operation Leaves and Feasible Regions

It is well known that the composition curves obtained from the numerical integration of Eqs. 10 and 11 terminate at a pinch point where there is no further change in composition.[2] At a pinch point the left-hand side of Eq. 10 vanishes and we must necessarily have $(x_E) = (x_L) = (x_P)$. As shown in the Appendix, the pinch-point composition is given by

$$(x_P - y^*) = -\frac{1}{r}(x_D - y^*) \tag{13}$$

The solution of Eq. 13 yields a parametric curve in composition space called the *pinch-point curve* (PPC) (see Wahnschafft et al.[3] and pp. 138–142 of Doherty and Malone.[2]). A similar relationship can be derived for the stripping section from Eq. 11. These relationships are independent of mass-transfer effects. Thus, composition profiles for both the equilibrium and nonequilibrium models possess the same set of pinch points. Castillo and Towler[6] came to the same conclusion, based on the observation of Agarwal and Taylor[5]—derived from column simulation calculations—that the true minimum reflux was independent of mass-transfer effects. As we will show below, we need to attach a caveat to the result of Agarwal and Taylor.[5] We can see from these theoretical considerations that the locus of pinch points (the PPC) is determined by the thermodynamics of the mixture and does not depend on mass-transfer effects independently of any statement about the minimum reflux or of any hardware choice.

The area between the pinch-point curve and the composition trajectory at total reflux is called the *operation leaf*.[6] All possible composition profiles are contained within the operation leaves. It is well known that for a feasible column the composition trajectories that originate from the distillate and bottom product composition must intersect. Thus, a feasible design requires that the operation leaf for the rectifying section overlap that for the stripping section. Because mass transfer can influence the location of the composition trajectories at total reflux[4,6,8] it follows that mass transfer may lead to nonequilibrium operation leaves that differ from those for the corresponding equilibrium model.

We illustrate with a simple example involving ethanol (1)–water (2)–acetone (3) as shown in Figure 3. The top row of figures is for an equilibrium model, whereas the bottom row is for a nonequilibrium model of a tray column with $Đ_{ref} = 1 \times 10^{-5}$, $C_1 = 0.65$, and $C_2 = 1$.

The specified feed and product stream compositions for the columns in Figure 3a are

$$(x_F) = (0.333, 0.333) \quad (x_D) = (0.061454, 0.238611)$$
$$(x_B) = (0.580496, 0.419445)$$

Not all of the product compositions are independent, of course; the unspecified values were computed from the overall material balances. The feed and product points are indicated by the black diamonds in Figure 3. However, note that the feasibility regions for the two models (the gray areas in Figure 3) are almost identical because they are determined by mass balance considerations and the feed pinch-point curve. The areas differ only slightly as a result of differences in the respective distillation boundaries caused by mass-transfer effects.

The composition profiles are shown as thin solid lines in Figure 3. The designs in Figure 3a are at a (specified) reflux ratio $r = 1$ and boil-up ratio $s = 1.81$ (the latter calculated from Eq. 1). We can see that a feasible design can be obtained with either model. The composition profiles for the equilibrium and the nonequilibrium models end at exactly the same pinch points. However, we can also see that the composition trajectories between their respective product and pinch points are different. These differences in curvature have an impact on the number of stages needed for the separation, as we shall see below.

Figures 3b and c show similar calculations for a column on the other side of the distillation boundary. The feed and product compositions for the columns in these figures are

$$(x_F) = (0.02, 0.546) \qquad (x_D) = (0.008, 0.092)$$

$$(x_B) = (0.03, 0.96)$$

The hatched areas in Figures 3b and c are the operation leaves constructed from the pinch-point curves and the composition profiles at total reflux ratio (residue curves and composition trajectories at total reflux). We observe that the operation leaves based on equilibrium and nonequilibrium models might be significantly different. The reason for this is the different shape of the composition profiles at total reflux and the residue curves (the pinch-point curve—one other border of the operation leaf—is the same for both models).

In Figure 3b we see that the pinch-point curve and the nonequilibrium ∞/∞ composition trajectory intersect. This occurs when mass-transfer effects are able to sufficiently change the curvature of the composition trajectory at total reflux (see also Castillo and Towler[6]). In this case we see that the equilibrium model suggests that a feasible design is possible, but the nonequilibrium model leads to the opposite conclusion. We can obtain a feasible design from both models if we increase the reflux ratio to 1.52, as shown in Figure 3c.

This illustration clearly shows that mass transfer has at best a marginal affect on the size and location of the feasible regions for a given feed. The product operations leaves, however, might differ significantly from those obtained with an equilibrium model. Furthermore, a boundary value design method might fail when a nonequilibrium model is used, although a feasible design was obtained with an equilibrium model. This does not mean that a column designed by an equilibrium model would not be able to meet its specifications. Obviously, the specified product compositions are fixed in the design method, but not for a real column. In most cases we will be able to meet the specifications simply by changing the operation point. This, however, results in higher energy costs. Later in this paper we will show that accounting for mass-transfer limitations might allow us to develop alternative designs.

Number of Stages and Feed Stage Location

The arc length of the composition profiles is related to the height of a section of packing in a packed column or approximately to the number of trays in a tray column. Mathematically speaking, the arc length ζ can be determined from

$$d\zeta = \sqrt{\sum_i \left(\frac{\partial x_i}{\partial \eta}\right)^2}\, d\eta \tag{14}$$

Substitution of the expressions for the composition trajectories in Eq. 14 will result in an algebraic relation between the arc length and the dimensionless column height. In practice, however, we determine the number of stages from

$$N_{stg,\mathrm{A}} = \int_0^{\eta_\mathrm{A}} d\eta \approx \eta_\mathrm{A} \tag{15}$$

where $N_{stg,\mathrm{A}}$ denotes the number of stages in column section $\mathrm{A} \in \{R, S\}$, where R and S refer to the rectifying and stripping sections, respectively. To estimate the number of theoretical (that is, equilibrium) stages we compute the average efficiency and multiply it by the actual number of stages. The average efficiency is estimated by the integral of the geometric average efficiency along the composition trajectory divided by the actual number of stages. Because we multiply and divide with the actual number of stages only the integral remains

$$N_{EQ,\mathrm{A}} \approx \int_0^{\eta_\mathrm{A}} \varepsilon(\eta) d\eta \tag{16}$$

where $N_{EQ,\mathrm{A}}$ denotes the theoretical number of theoretical stages in column section A.

The integration starts from a product point in composition space and ends at the composition on the feed stage. To locate the latter points we make use of the material balance for the liquid phase on the feed stage (assuming a saturated liquid feed)

$$\frac{r}{r+1}(x_R - x_F) = \frac{s+1}{s}(x_S - x_F) \tag{17}$$

where (x_R) is the liquid composition leaving the rectifying section and (x_S) is the liquid composition entering the stripping section. Equation 17 implies that the points corresponding to that of composition of the liquid leaving the rectifying section and that of the composition of the stream entering the stripping section are collinear, with the point representing the composition of the feed. The points of intersection of a straight line through the feed composition and that satisfy Eq. 17 correspond to (x_S) and (x_R). Once (x_S) and (x_R) are known we can determine the integration length in the stripping section η_S and that in the rectifying section η_R.

We now return to our illustration with the ethanol (1)–water (2)–acetone (3) system discussed above. The differences in curvature of the composition trajectories shown in Figure 3 are

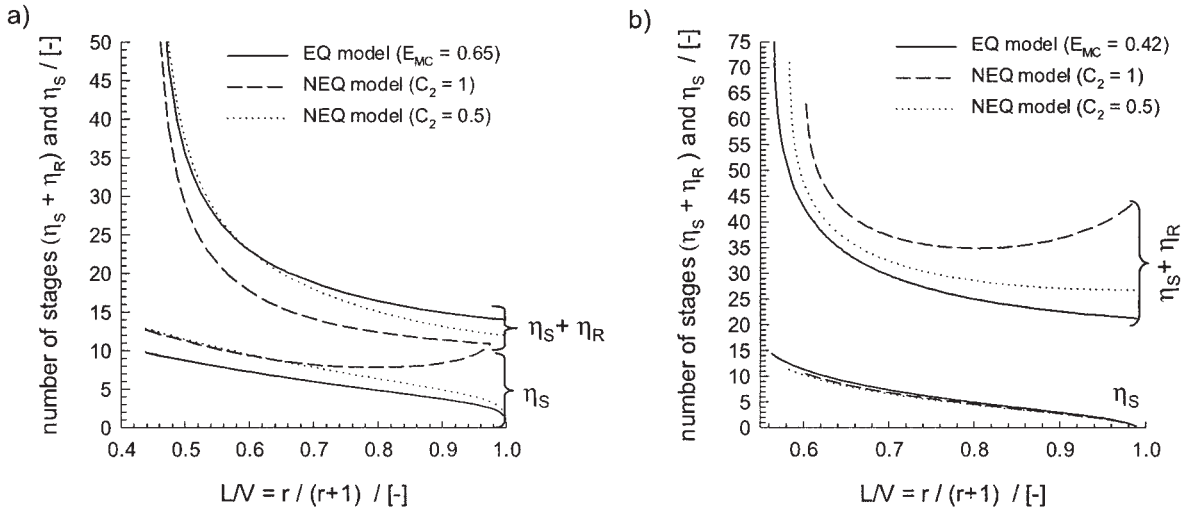

Figure 4. Estimate of the number of stages for varying reflux rate.

Feed and product stream compositions are as in Figure 3. For the binary NTUs we used the parameters $C_1 = 0.65$ and $Đ_{ref} = 10^{-5}$ m^2/s.

reflected in the lengths of the composition trajectories and, therefore, in the number of stages. For our column in the distillation region close to pure water (Figure 3a) we observe that the equilibrium model needs 36 stages, whereas the nonequilibrium model requires just 29 stages (trays). Moreover, the equilibrium model suggests that the feed stage should be 9 stages (or 25%) from the bottom, whereas the nonequilibrium model suggests that the feed should be 11 stages (or 38%) from the bottom. On the other hand, if we compute the number of stages in the distillation region close to pure ethanol (Figures 3b and c) we see that the equilibrium model predicts a requirement for fewer stages than does the nonequilibrium model.

Figure 3 also shows that the conceptual designs have been validated with the column simulation model ChemSep,[10] using a mass-transfer model as in Eq. 8 where feed composition, number of stages, reflux ratio, and boil-up ratio were specified. In both equilibrium and nonequilibrium model simulations the predicted product compositions are in very close agreement with values specified in the original design problem.

Figure 4 shows the total number of stages ($\eta_S + \eta_R$) and feed location (η_S) as a function of the internal flow rate, L/V. Figure 4a is for a column in the distillation region of pure water (see also Figure 3a) and Figure 4b is for a column in the distillation region close to pure ethanol. Two slightly different versions of the nonequilibrium model are compared to the equilibrium model. In nonequilibrium model I the exponent C_2, in the binary NTU correlation,[8] is 1 and for model II it is 0.5. The constant for the binary NTUs is $C_1 = 0.65$ in both models. The reference diffusivity is chosen to be 10^{-5} m^2/s. Thus, the relative diffusivities—the ratio of the reference diffusivity and the binary Maxwell–Stefan diffusivities—are >1 for most binary pairs. This leads to the binary NTUs being larger for model I than for model II, where we evaluate the square root of the relative diffusivities. The multicomponent efficiencies for model I are, therefore, higher than those for model II. For a design in the distillation region close to pure water we find that the equilibrium model requires *more* stages than do either of the nonequilibriuim models, although the efficiency used in the equilibrium model is significantly larger ($\varepsilon = 0.65$) than that estimated for either NEQ model I ($\varepsilon = 0.55$) or model II ($\varepsilon = 0.5$). We observe exactly the opposite trend in Figure 4b for the distillation region close to pure ethanol. In this case the efficiencies are all close to 0.42 (see Figure 5b in Taylor et al.[8]). The equilibrium model requires fewer stages than either nonequilibrium model. Even more interestingly, we find that the nonequilibrium model I requires *more* stages than the NEQ model II.

Strictly speaking, the length of the trajectories in composition space is not equivalent to the number of stages. Nevertheless, a comparison of the NEQ model composition trajectories with that for an equilibrium model leads to the explanation. From Figure 3 we can see that mass transfer causes the trajectories to follow longer paths in the distillation region close to pure ethanol, whereas mass transfer leads to shorter paths in the distillation region close to pure water. The change in curvature of the composition trajectories attributed to mass transfer leads to different total numbers of stages and feed locations. These observations demonstrate clearly that the angle between the driving force and actual composition change on a stage (see Figure 2a) is the cause of what can be significant design differences.

Figure 4 also illustrates the well-known result that the number of stages needed for a specified separation increases as the reflux ratio decreases and becomes infinite when the reflux ratio is at its minimum and where the design has the lowest energy demand. The upper limit is the maximum reflux ratio. Because we account for the material balance around the feed, this maximum reflux is in general finite, except for the special case where both products are lying on the same composition trajectory at total reflux. The maximum reflux ratio is associated with the minimum number of stages required to achieve the desired separation. Indeed for the equilibrium model and nonequilibrium model II we observe that the minimum number of stages occurs at the maximum reflux, as can be seen in Figure 4b. However, if we account for larger differences between the component efficiencies by using the NEQ model I, we observe that the minimum number of stages is reached at $r/(r + 1) \approx 0.8$ and not at its maximum reflux ratio.

It is clear from this case study that the optimal number of stages and feed location can be different for nonequilibrium and equilibrium models. Simply using the equilibrium model for design runs the risk of producing a suboptimal design. In this case a more costly design might be the result.

Minimum Reflux

The composition trajectories curves obtained from the numerical integration of Eqs. 10 and 13 terminate at a pinch point where there is no further change in composition. A feasible design exists if the composition trajectories in the rectifying and stripping section intersect before the pinch point is reached.[2] If the trajectories do not intersect the reflux ratio is too low and no column can be designed that can produce the desired products. The column is operating at minimum reflux when one of the composition trajectories just touches the other composition trajectory.[2,11]

Agarwal and Taylor[5] found by simulation that the minimum reflux is the same for both equilibrium and nonequilibrium models. This result (if true) means that existing methods of estimating the minimum reflux based on equilibrium models (see, for example, Doherty and Malone,[2] Koehler et al.,[12] and Tanskanen and Pohjola[13]) remain useful. In what follows we shall show that the minimum reflux ratios found from the equilibrium and nonequilibrium models are the same only under certain conditions (that were not fully appreciated by Agarwal and Taylor[5]).

One way to determine the minimum reflux ratio is to numerically integrate the composition profiles in the rectifying and stripping section at different reflux (and reboil) ratios until we find a value of r (and s) for which one of the profiles just touches the other. Our approach is similar, but we make use of the pinch-point curves and, usually, only one composition profile needs to be integrated. As shown in the following example common sense will allow us to determine a priori the section in which a pinch might occur. Once we know the pinch-point curve of interest, we can numerically integrate the composition profile in the other section assuming a certain boil-up or reflux ratio. After integration we determine the intersection with the pinch-point curve. The value of the boil-up or reflux ratio in the nonpinched section has to correspond to reflux or boil-up ratio at the pinch point. Equation 1 relates the reflux and boil-up ratio in the pinched and nonpinched section. We vary the reflux ratio and integrate composition profiles in the nonpinched section until Eq. 1 is satisfied. We use a simple search algorithm until the condition for minimum flow is satisfied (the pinched profile just touching the other trajectory).

Assuming that one of the composition profiles is touching the other one is "only" a very good method for determining an approximate value of the minimum reflux ratio. However, this procedure does not account for the feed. To do so it is most convenient to revisit the lever rule given by Eq. 17, which contains only three unknowns—(x_R), (x_S), and r—given that the boil-up ratio and the reflux ratio are related by the total mass balance. Now, if we consider that a pinch point emerges in the rectifying section we know that the composition leaving the section equals the pinch-point composition $[(x_R) = (x_P)]$ and that the reflux ratio for that composition point is the one that belongs to that specific pinch point [that is, $r = r(x_P)$]. We can compute the composition entering the stripping section for any pinch point by solving Eq. 17 for (x_S). In practice this allows us to transform the pinch-point curve in the rectifying section into a curve of compositions entering the stripping section (SCC)

$$(x_S) = \frac{s(x_P)r(x_P)}{[r(x_P)+1][s(x_P)+1]}(x_P - x_F) + (x_F) \quad (18)$$

We may also derive an expression for the composition leaving the rectifying section (RCC) by solving Eq. 17 for (x_R) and substituting the pinch-point curve in the stripping section

$$(x_R) = \frac{[r(x_P)+1][s(x_P)+1]}{s(x_P)r(x_P)}(x_P - x_F) + (x_F) \quad (19)$$

We illustrate the use of the SCC and the RCC in what follows.

We have used this procedure for the calculation of the minimum reflux to the *n*-hexane/*n*-heptane/*n*-nonane system. Thermodynamic properties were calculated with the Peng–Robinson equation of state. The binary NTUs were estimated from Eq. 8 with the reference diffusivity fixed at 3×10^{-6} m^2/s, $C_1 = 1.5$, $C_2 = 0.5$. The geometric average efficiency for this system varies over a very narrow range, from 0.8 to 0.84. Furthermore, we see from Figure 2b that the angle between the driving force and the actual composition change is rather small and does not exceed approximately 2°. Thus, the individual component efficiencies will have nearly the same value. Under such circumstances, we do not expect visible differences between nonequilibrium and equilibrium composition trajectories.

The feed composition is specified with $x_{C6,F} = 0.3$ and $x_{C9,F} = 0.4$. We choose a bottom product composition of $x_{C6,B} = 0.001$ and $x_{C9,B} = 0.5711$. Figure 5a shows the composition space if we aim for a hexane purity of 99.9% and a nonane mole fraction of 10^{-6} in the distillate. These specifications are closely related to the ones used by Levy et al.[11] and Agarwal and Taylor.[5] The upward-hatched area denotes the feasible region for rectifying composition profiles and the downward-hatched area is the feasible region for the stripping composition profiles. It can be seen that the operation leaf of the stripping section overlaps completely with that of the rectifying section. The modified pinch-point curves, RCC and SCC, are plotted with dashed lines in Figure 5a. We immediately see that the modified pinch-point curve SCC does not cross the operation leaf for the stripping section. Thus, no pinch is expected to emerge in the rectifying section. The modified pinch-point curve of the stripping section (RCC), however, does cross the operation leaf of the rectifying section and so a pinch in the stripping section might be expected.

Figure 5b shows the result of the search for the minimum reflux. The pinch-point composition equals the composition of the stream entering the stripping section and lies on a straight line with the feed and composition leaving the rectifying section. Thus, the mass balance around the feed is satisfied. Furthermore, we see that the RCC intersects the composition profile in the rectifying section exactly at a reflux ratio of 2.84. This is the minimum reflux ratio for this design with a nonequilibrium model. If we do not account for mass transfer ([Ω]

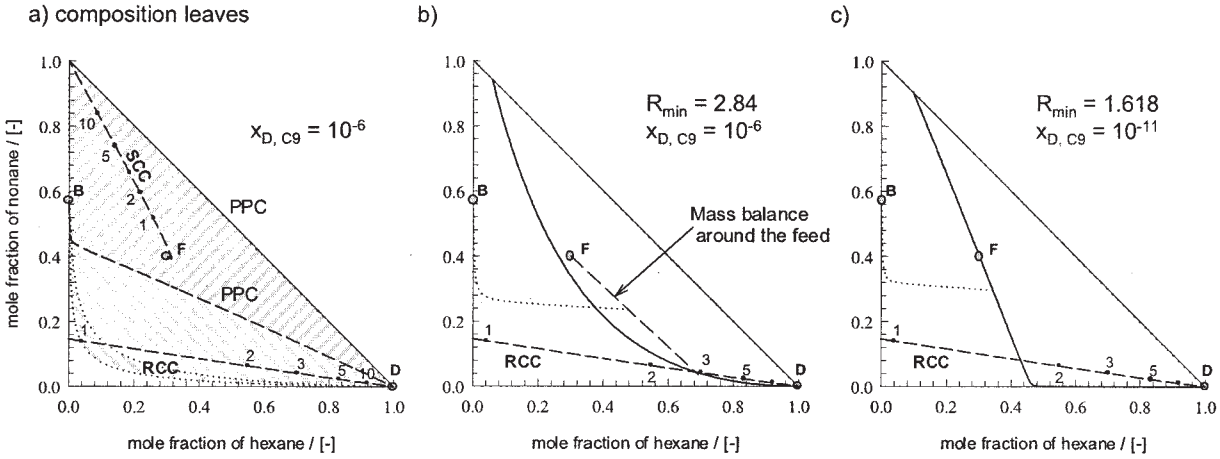

Figure 5. Minimum reflux case study for a mixture of hexane (1)–heptane (3)–nonane (2).

(a) Operation leaves for a nonane distillate purity of $x_{D,[infi]C9} = 10^{-6}$. RCC and SCC are the rectifying and stripping composition curves (see text). (b) Composition profiles at minimum reflux for $x_{D,[infi]C9} = 10^{-6}$ and $x_{D,[infi]C9} = 10^{-11}$. Feed and bottom product stream compositions are $(x_F) = (0.3, 0.4)$ and $(x_B) = (0.001, 0.419)$. Mass-transfer model is based on a model for trays ($Đ_{ref} = 3 \times 10^{-6}$ m^2/s, $C_1 = 1.5$, and $C_2 = 0.5$).

$= [I]$), then the minimum reflux ratio increases to 3.04. The slight difference in the values of the minimum reflux ratio is explained by the fact that even slightly different component efficiencies can change the curvature of the composition trajectories. In Figure 5c we tighten the specification of nonane in the distillate to a mole fraction of 10^{-11} and the minimum reflux ratio, found with both nonequilibrium and equilibrium models, is 1.618.

Figure 6 shows how the calculated minimum reflux ratio varies with the specified mole fraction of nonane in the distillate for the same bottom and feed compositions. All models exhibit the identical minimum reflux ratio for very sharp splits, as observed by Agarwal and Taylor.[5] This is caused by the topology of the singular points. In very sharp splits the composition trajectories closely follow the boundaries between

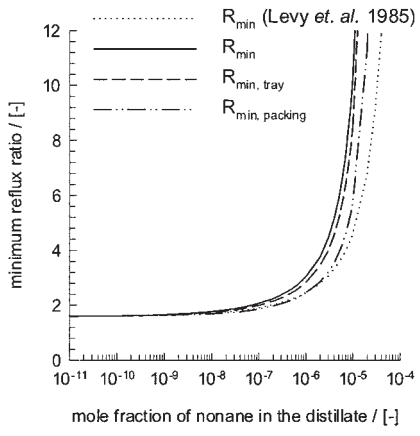

Figure 6. Minimum reflux ratio for the separation of the hexane (1)–heptane (3)–nonane (2) mixture when the distillate purity of nonane is varied without changing the feed and bottom product stream compositions.

Further specifications can be found in Figure 4. The figure also includes the minimum reflux ratio for a packed tower ($Đ_{ref} = 3 \times 10^{-6}$ m^2/s, $C_1 = 1.0$, and $C_2 = 0.6667$).

singular points, as seen in Figure 5b. Doherty and Malone[2] pointed out that the saddle of the rectifying profile, the feed composition, and the stable node in the stripping section (pinch point) are collinear. The composition trajectory closely follows this straight line and so the criterion of touching composition trajectories is sufficient to determine the minimum reflux. According to Doherty and Malone[2] (see p. 147), this observation also holds for highly nonlinear mixtures. In the previous section we already showed that the location of a singular point (such as pinch point) is independent of mass transfer. Thus, the differences between an equilibrium model and nonequilibrium model are negligible. Figures 5b and 6 confirm this observation.

On the other hand, Figure 6 also shows large differences in the minimum reflux for less sharp splits. In these cases the curvature of the composition trajectories is changed by mass transfer, only slightly, but enough to influence the minimum reflux ratio. Furthermore, the intersections of the composition trajectories and the RCC are located close to the distillate product, as can be seen in Figure 5. The reflux ratio in this part of the RCC is increasing rapidly toward infinity. Thus, it is not a surprise that the minimum reflux ratio is also highly sensitive, and we should be aware of this effect when designing a column. We shall explore much more severe consequences of mass-transfer effects in what follows.

Overlap Regions

We consider now a design problem posed by Doherty and Malone.[2] They call this example the "DeRosier Problem," after the student who first developed a successful design. The first part of the problem calls for the design of a column to separate a feed of 20 mol % isopropanol, 40 mol % methanol, and 40 mol % water. The bottom product is to contain 0.5 mol % methanol and the distillate is to contain 99 mol % methanol and 0.5 mol % water. Doherty and Malone[2] used the NRTL equation to describe the VLE for this system. We have used the UNIQUAC equations in our calculations (Pelkonen et al.[14] validated the latter model with extensive experimental data).

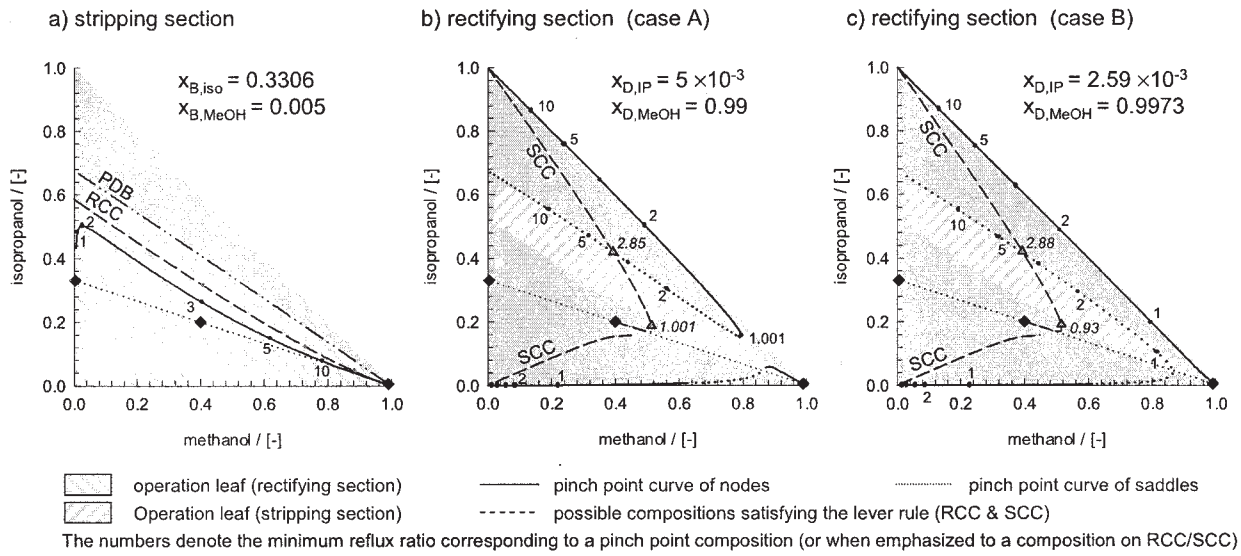

Figure 7. Pinch point, PDB, SCC, and RCC curves for a mixture of methanol (1)–isopropanol (2)–water (3).

If not specified, the feed and product stream compositions are (x_B) = (0.3306, 0.005), (x_D) = (0.005, 0.99), and (x_F) = (0.4, 0.2). Hatched area denotes the operation leaves of (a) the distillate and (b–c) the bottom product stream.

The solution of this design problem appears straightforward. The residue curve map and composition angle map for this system are shown in Figure 2c. The first step is to determine the minimum reflux. We can limit our search by reasoning on what branch of the stable pinch-point curves (the SCC and RCC) might contain the actual solution. Figure 7a shows the operation leaf for the bottom product compositions. The feasible region of the rectifying section for the distillate composition close to pure methanol is the distillation region methanol–water–azeotrope, subsequently called the distillation region of pure water. The RCC lies in that region and thus pinch points in the stripping section might occur. When focusing on pinch points in the rectifying section we have to distinguish between two possible scenarios:

(A) A continuous pinch-point branch from pure methanol to pure water (see Figure 7b)

(B) A continuous pinch-point branch from pure methanol to pure isopropanol (see Figure 7c)

Which of these applies to the design at hand depends on the location of the desired distillate. The pitchfork bifurcation distillation boundary (PDB) shown in Figure 7a divides the composition space in two regions. If the distillate composition is lying on the side of pure water, then the pinch-point topology resembles Figure 7b. On the other hand, if it is lying in the region of pure isopropanol the topology will look similar to that shown in Figure 7c. In the present case study, however, we can eliminate any pinch point in the stripping section. An intersection of SCC with the stripping section composition profile for the specified bottom product requires a minimum reflux < 3. As can easily be seen from Figure 7a all stripping section composition trajectories with a corresponding reflux ratio of <3 will end up in a pinch point before they possibly can intersect with the SCC. Therefore, we can restrict our search for the minimum reflux ratio to a single branch of the RCC.

The PDB describes the limiting case of the pinch-point topology for which the pinch-point branches will touch. It is important to remember that, because the pinch-point topology is not influenced by mass-transfer effects, the PDB will be valid for any mass-transfer model. Figure 8a shows the PDB along with the distillation boundaries (DB) for an equal diffusivity model (RC), a tray column, and a packed tower. The PDB and the RC distillation boundary almost coincide. Thus, the area between the PDB and RC–DB, the so-called *overlap region*, is vanishingly small. According to Doherty and Malone[2] this implies that the RC–DB cannot be crossed in practice and so it is unlikely that the rectifying composition trajectory exhibits a bifurcation. A consequence is that a design based on an equal-diffusivity mass-transfer model will fail if the desired distillate composition is in the region of pure isopropanol.

We carried out minimum reflux calculations for two different water distillate purities. Figure 8b shows the successful design for an equal diffusivity model at a minimum reflux of 3.08 and at a mole fraction of water in the distillate 2.16×10^{-3}. Decreasing the water mole fraction to 9.8×10^{-5} relocates the distillate composition in the PDB region of pure isopropanol, as can be seen in Figures 8a and c. As might now be expected, the design fails. However, a packed tower design is successful, for which the minimum reflux ratio is found to be 3.08, as shown in Figure 8c. If the water purity is lowered, however, the minimum reflux ratio for the packed tower is much higher (20.3) than that for the equal diffusivity model. The reason for this is shown in Figure 8a. Because mass-transfer effects influence the distillation boundary, we observe a wider overlap region and so a design can be successful for high water purities without significantly increasing the methanol purity.

Figure 9 shows how the minimum reflux changes with the mole fraction of water in the distillate. For a fixed feed and bottom product composition we observe for four different mass-transfer models that a larger overlap region close to pure methanol that allows higher water purities (see Figure 8a). For tray model I, the binary NTUs depend on the square root of the diffusivities, whereas they are directly proportional for model II. As a result, the distillation boundary for tray model I is less

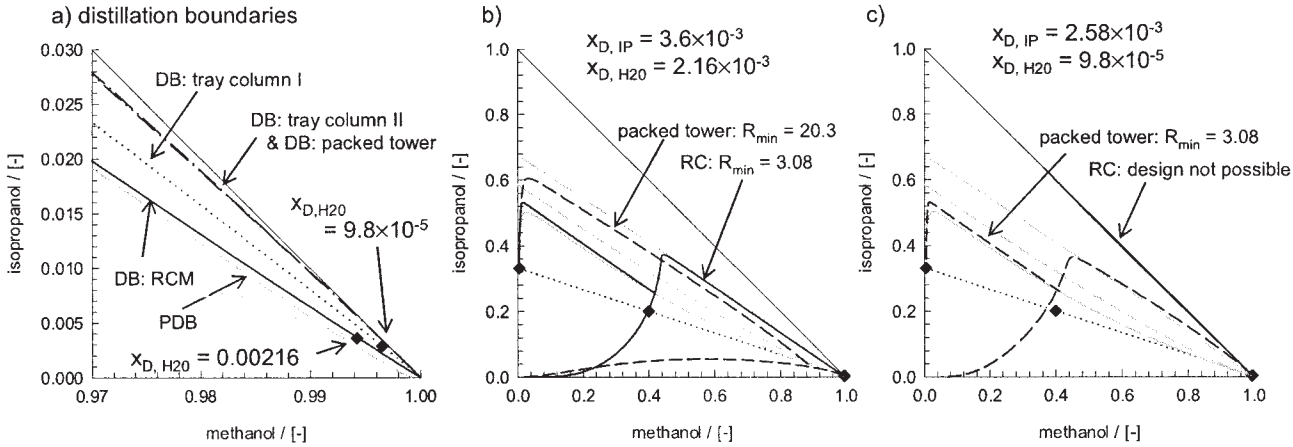

Figure 8. (a) Distillation boundaries close to pure methanol for four different MT models: RC (equal diffusivity model), tray column I ($C_1 = 1.1$, $C_2 = 0.5$), tray column I ($C_1 = 0.5$, $C_2 = 1$), packed tower ($C_1 = 0.6$, $C_2 = 0.6667$) (for all models, $\mathcal{D}_{ref} = 5 \times 10^{-5}$ m^2/s); (b–c) composition profiles at minimum reflux for the packed tower and the equal diffusivity model. Light gray lines refer to the RRC and the pinch-point curves in Figure 6.

curved than that for model II. Therefore, following our previous argument, the minimum attainable water purity is much higher for model I than it is for model II. However, Figure 9 shows that the absolute minimum reflux ratio is close to 3 for all models. These results are in agreement with our observations of the paraffin system. In the limiting case of very sharp splits the composition trajectories closely follow the distillation or composition space boundaries before they hit a saddle point. Thus, as discussed by Doherty and Malone,[2] their behavior is dictated predominantly by the pinch-point topology. The influence of the distillation boundaries is not noticeable and the limiting reflux ratio remains the same for any model [also see the composition trajectories for the designs ($r_{min} = 3.08$) in Figure 8b].

What we can learn from Figure 9 is that, although the minimum reflux is the same, the maximum attainable water purity is not when mass-transfer effects play a role. This brings us back to the exercise in Doherty and Malone.[2] After designing the column they ask the students to reduce the water content in the distillate stream down to 50 ppm to avoid catalyst poisoning. Their solution is to redesign the column and increase the methanol purity to 99.99 mol %. Figure 9 shows, however, that water impurities can be reduced down to 93 ppm without any additional effort. A redesign does not require methanol purities of 99.99 mol %. Moreover, it is still possible to design a suitable column without changing the bottom product composition at all. The distillation boundary for a packed tower in Figure 8a shows that water can be removed almost entirely from the distillate without leaving the distillation region of pure water. On the other hand we know from the location of the PDB that, for low reflux ratios, the composition trajectories in the rectifying section will end on the continuous pinch-point curve that goes from pure methanol to pure isopropanol. Thus, at a certain reflux ratio a bifurcation will take place. This is shown in Figure 10. For a reflux ratio of 10 the composition trajectory will end at a pinch point that is located in the distillation region of pure isopropanol. Thus, a column design fails. On the other hand, if we increase the reflux ratio

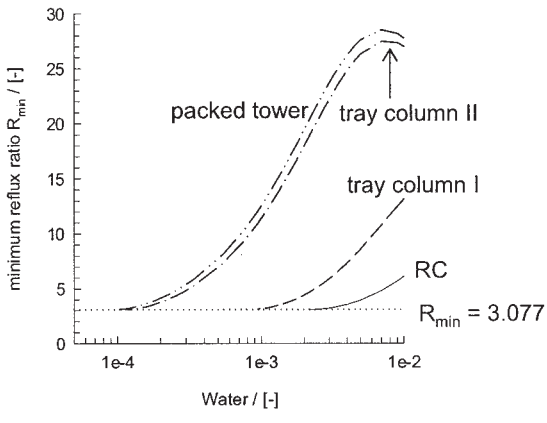

Figure 9. Minimum reflux ratio when the distillate purity of water is varied.

Data for the MT models and the specified column stream compositions are given in Figures 6 and 7.

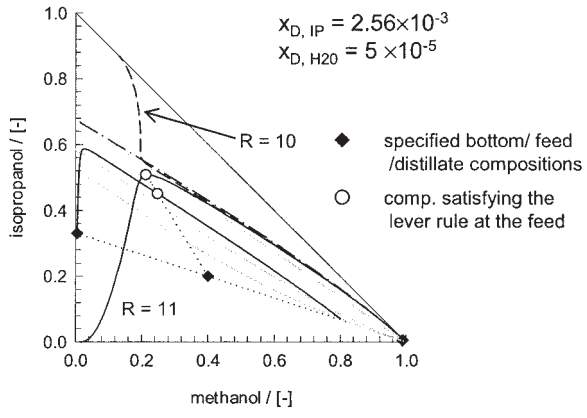

Figure 10. Column design study for a packed tower with a specified water purity of 50 ppm in the distillate.

Design for a packed tower ($C_2 = 0.6667$) is possible for $r = 11$. For lower reflux ratios, say $r = 10$, the design will fail.

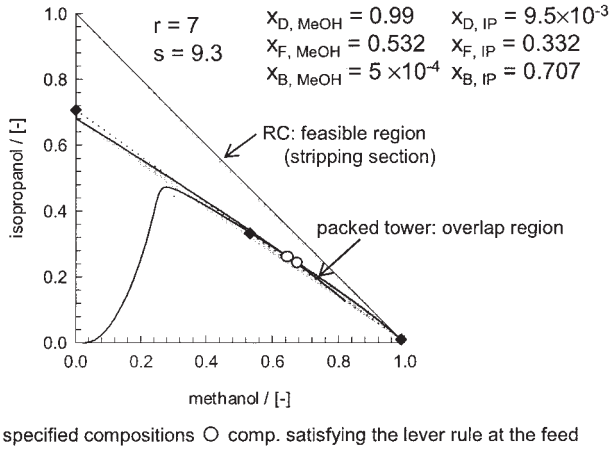

Figure 11. Column design for a packed tower (C_2 = 0.6667) that crosses the distillation boundary.

Additional overlap region attributed to mass-transfer limitation is marked in gray.

up to 11 we successfully obtain a column design and reach our specification with a methanol purity of only 99.74 mol %.

We must note that there exists extensive experimental evidence for mass-transfer effects for this system in a packed tower and we know that nonequilibrium models accurately describe their behavior.[15] This example from the text of Doherty and Malone[2] demonstrates that, although the limiting value of the minimum reflux is the same, the predicted amounts of trace components in a product stream can be very different. It is, therefore, particularly important to use mass-transfer models when trace components are a concern.

It is reasonable to ask whether our neglect of the resistance to mass transfer that resides in the liquid phase could affect these results. To test this we have modeled this operation using the nonequilibrium model in ChemSep,[10] both without and with the liquid-phase resistance (with liquid-phase mass-transfer coefficients estimated from a penetration model). The column profiles were essentially identical in both cases, indicating that the liquid-phase resistance was not significant here (but that is not to say that it might not be important in other examples).

In the preceding material we made use of the overlap region (the area between the distillation boundary and the pitchfork distillation boundary) to exploit mass-transfer effects so as to obtain a high purity product. According to Doherty and Malone,[2] a composition in the overlap region can be obtained from a feed composition in either distillation region. For an equal-diffusivity model (RC) the overlap region is vanishingly small. However, for a packed tower we observe a reasonably large overlap region resulting from the additional curvature of the distillation boundary. Thus, it should not be a surprise that we are able to cross the distillation boundary with a packed column. An example for such a design is given in Figure 11. In industrial practice such a design, however, would not be considered unless all other alternatives have been explored.

Finally, we consider a system with a strongly curved distillation boundary, the acetone–benzene–chloroform mixture shown in Figure 1d. As shown in Figure 12a and extensively discussed by Doherty and Malone,[2] the overlap region for this system is rather large and allows a column design that crosses the distillation boundary. Mass-transfer effects, however, further increase the curvature of the distillation boundary and so narrow the overlap region. We illustrate this by choosing a bottom product composition in Figures 12b and c that lies in the overlap region of the RCM but not in the overlap region of a CTM for a packed tower. Figure 12b shows that the equal diffusivity model (RC) exhibits a bifurcation at a boil-up ratio > 7. The model for the packed tower does not exhibit a bifurcation at all (see Figure 12c). Therefore, such a bottom product composition could not be used to purify chloroform. In this particular case study, however, a column design would aim for pure acetone and for a binary mixture of benzene and methanol

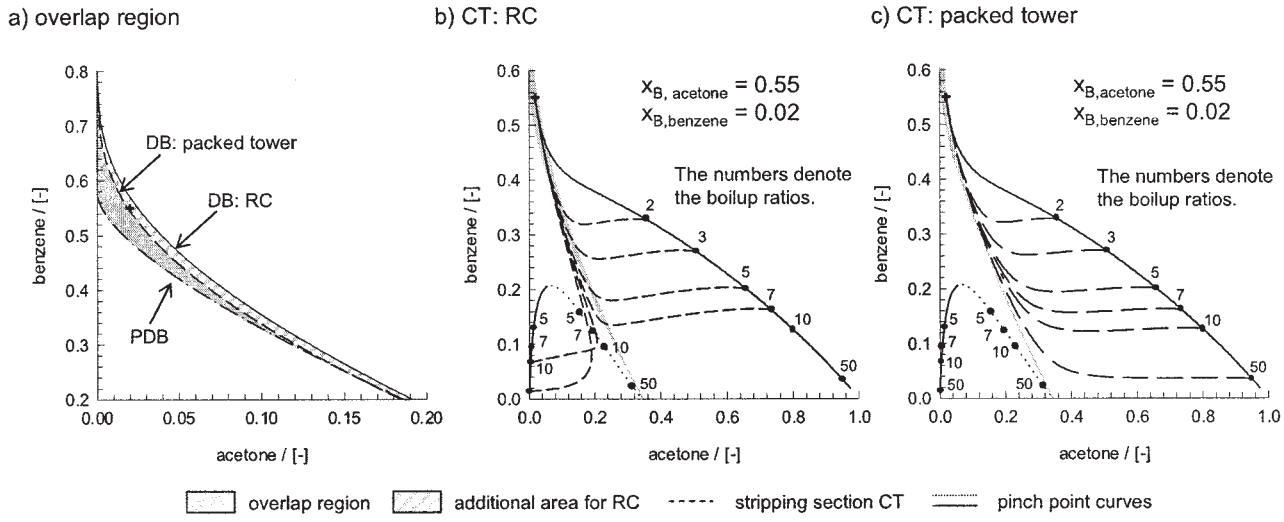

Figure 12. Column design for separating an acetone (1)–benzene (2)–chloroform (3) mixture.

Gray and hatched area in (a) shows the overlap region for an equal-diffusivity model. The gray area itself marks the narrowed overlap region arising from mass-transfer limitation. (b–c) Pinch-point curves and composition profiles for a fixed bottom product composition for packings with (b) an equal diffusivity model and (c) a NTU model ($Đ_{ref} = 6 \times 10^{-6}$ m^2/s, $C_1 = 1.5$, and $C_2 = 0.6667$). Numbers indicate the boil-up ratio corresponding to the indicated pinch point.

and the effect of a narrowed overlap region does not come into play (for more details see Doherty and Malone[2]). The point here is that mass-transfer effects can lead to a design failure if the overlap region is narrowed.

Conclusions

In this paper we have considered the influence of mass transfer on distillation column design. Our conclusions are as follows:

- The column design equations incorporating mass-transfer effects are similar to the conventional design equations, differing only in the inclusion of a matrix of coefficients that is a function of the binary numbers of transfer units. This coefficient matrix can be estimated using simple mass-transfer models that require knowledge of the binary diffusivities and two parameters that can easily be estimated from binary Murphree efficiencies.
- The modified design equations are easy to solve numerically. The inclusion of mass-transfer effects increases the computational cost by a trivial amount.
- Mass-transfer effects do not change the steady-state topology. Pinch-point curves and pitchfork distillation boundaries are invariant. Mass transfer does change the composition trajectories, which might, therefore, cross the pinch-point curves. As a consequence, a feasible design based on mass transfer consideration might be rejected by a design method based on residue curves. The converse is also true.
- Inclusion of mass transfer in the design equations allows us to estimate the actual number of stages (or the column height). The geometric average efficiency is useful for obtaining a better estimate of the number of stages. We have noticed that the curvature of composition trajectories has a significant impact on the total number of stages and on the feed stage location. Thus, nonequilibrium composition trajectories can help in the early stages of column design.
- Mass-transfer effects do not influence the minimum reflux for columns involving a very sharp split. This is because the corresponding composition trajectories closely follow the distillation boundaries and the process is influenced predominantly by the thermodynamic topology of the system. However, mass-transfer effects may strongly affect the minimum reflux for less than very sharp separations.
- Mass-transfer effects can have a significant impact on the amounts of trace components in product streams. Mass transfer should be taken into consideration when trace components are a concern. It is not inconceivable that the exploitation of mass-transfer effects can lead to a cheaper design.
- Mass-transfer effects can create or widen an overlap region. Consequently, designs that cross equilibrium distillation boundaries might be possible.
- Mass-transfer effects can also narrow an overlap region for systems where the residue curve map exhibits a curved distillation boundary. Designers should thus be aware that a design might fail if mass-transfer effects play a significant role.
- Mass-transfer effects are more likely to be significant if the binary diffusion coefficients of the binary pairs are very different from one another.

Notation

C = numerical constants
$\mathcal{D}$ = Maxwell–Stefan diffusion coefficient, m^2/s
L = molar liquid flow rate, mol/s
n = number of components
$\mathcal{N}$ = number of transfer units for a binary system
N_{stg} = number of stages
$[\mathbb{N}_{OV}]$ = matrix of overall multicomponent number of transfer units
$[Q]$ = matrix defined by Eq. 6
r = reflux ratio
s = reboil ratio
V = molar vapor flow rate, mol/s
x_i = mole fraction of component i in liquid phase
y_i = mole fraction of component i in vapor phase
y_i^* = vapor mole fraction of component i in equilibrium with liquid
z_i^α = mole fraction i in phase α

Greek letters

Δ = difference operator
ε = geometric average efficiency
ζ = arc length
η = dimensionless length coordinate
Λ = ratio of vapor to liquid flows
$[\Omega]$ = matrix defined by Eqs. 5 to 7

Superscripts

L = liquid-phase quantity or property
V = vapor-phase quantity or property
$+$ = property of virtual (reference) column in which all species have an equal facility for mass transfer

Subscripts

E = entering
i, j, k = component number
L = leaving
P = pinch point
R = rectifying section
S = stripping section

Matrix notation

$[\,]$ = square matrix of order $n - 1$
$[\,]^{-1}$ = inverse of a square matrix
$(\,)$ = column matrix of dimension $n - 1$

Acronyms

CT(M) = composition trajectory (map)
DB = distillation boundary
EQ = equilibrium
NEQ = nonequilibrium
PDB = pitchfork distillation boundary
RCC = rectifiying composition curve
RC(M) = residue curve (map)
SCC = stripping composition curve

Literature Cited

1. Seader JD, Henley EJ. *Separation Process Principles*. New York, NY: Wiley; 1998.
2. Doherty MF, Malone MF. *Conceptual Design of Distillation Systems*. New York, NY: McGraw-Hill; 2001.
3. Wahnschafft OM, Koehler JW, Blass E, Westerberg AW. The product composition regions of single-feed azeotropic distillation-columns. *Ind Eng Chem Res* 1992;31:2345-2362.
4. Taylor R, Krishna R, Kooijman H. Real-world modeling of distillation. *Chem Eng Prog* 2003;98:28-39.
5. Agarwal S, Taylor R. Distillation column design calculations using a nonequilibrium model. *Ind Eng Chem Res* 1994;33:2631-2636.
6. Castillo FJL, Towler GP. Influence of multicomponent mass transfer on homogeneous azeotropic distillation. *Chem Eng Sci* 1998;53:963-976.

7. Castillo FJL, Thong DYC, Towler GP. Homogeneous azeotropic distillation. 1. Design procedure for single-feed columns at nontotal reflux. 1998;37:987-997.
8. Taylor R, Baur R, Krishna R. Influence of mass transfer in distillation: Residue curves and total reflux. *AIChE J* 2004;50:3134-3148.
9. Taylor R, Krishna R. *Multicomponent Mass Transfer*. New York, NY: Wiley; 1993.
10. Kooijman HA, Taylor R. *The ChemSep Book*. Norderstedt, Germany: Books on Demand; 2001. (Available at http://www.chemsep.org)
11. Levy SG, Van Dongen DB, Doherty MF. Design and synthesis of homogeneous azeotropic distillation. 2. Minimum reflux calculations for nonideal and azeotropic columns. *Ind Eng Chem Fundam* 1985; 24:463-474.
12. Koehler J, Poellmann P, Blass E. A review on minimum energy calculations for ideal and nonideal distillations. *Ind Eng Chem Res* 1995;34:1003-1020.
13. Tanskanen J, Pohjola VJ. Minimum internal recycle in nonideal homogeneous multicomponent distillation. *Chem Eng Sci* 2000;55:2713-2726.
14. Pelkonen S, Kaesemann R, Gorak A. Distillation lines for multicomponent separation in packed columns: Theory and comparison with experiment. *Ind Eng Chem Res* 1997;36:5392-5398.
15. Pelkonen S, Gorak A, Ohligschlager A, Kaesemann R. Experimental study on multicomponent distillation in packed columns. *Chem Eng Process* 2001;40:235-243.

Appendix: The Pinch-Point Curve Equation

At a pinch point Eq. 10 reduces to a nonlinear set of equations

$$(0) = [\Omega](z) \qquad \text{where}$$

$$(z) = \left[(x_L) - \frac{r+1}{r}(y^*) + \frac{1}{r}(x_D) \right] \quad \text{(A1)}$$

The coefficient matrix $[\Omega]$ is a function of composition.[8] We also know that the matrix $[\Omega]$ is positive definite with real, positive eigenvalues $\lambda_i > 0$.[9] Now consider the quadratic form of Eq. A1

$$0 = (z)^T[\Omega](z) \quad \text{(A2)}$$

We know from matrix calculus that there exists a matrix $[P]$ for which $[P]^T[\Omega][P]$ yields a diagonal matrix with diagonal elements that are the eigenvalues of the matrix $[\Omega]$. Applying the transformation $(z) = [P](y)$ to Eq. A2 results in the quadratic form

$$0 = (y)[P]^T[\Omega][P](y) = \lambda_1 y_1^2 + \lambda_2 y_2^2 + \cdots + \lambda_{n-1} y_{n-1}^2 \quad \text{(A3)}$$

where the λ_i are the eigenvalues of $[\Omega]$. Because all of the eigenvalues are positive we know that only the trival solution $y_i = 0$ will satisfy Eq. A3. Thus, Eq. A1 also possesses only a trivial solution, $z_i = 0$, and what remains is a set of nonlinear equations

$$(z) = \left[(x_L) - \frac{r+1}{r}(y^*) + \frac{1}{r}(x_D) \right] = (0) \quad \text{(A4)}$$

the solution of which is Eq. 13.

Manuscript received Apr. 1, 2004, and revision received Jun. 15, 2004.